



NATURALLY OCCURRING CLAY, MONTMORILLONITE, AS A DRUG DELIVERY VEHICLE FOR IN VITRO EXTENDED RELEASE OF VENLAFAXINE HYDROCHLORIDE

Shilpa Jain^[a] and Monika Datta^{[a]*}

Keywords: Venlafaxine hydrochloride; montmorillonite; oral drug delivery

In the present work, a naturally occurring smectite group clay mineral, montmorillonite, (Mt) has been explored as a vehicle for delivery of an antidepressant drug Venlafaxine hydrochloride, VF. The effect of pH of the drug solution, time and initial drug concentration on drug loading capacity of Mt has been studied. The adsorption isotherm was fitted by the Langmuir model and follows the pseudo-second-order kinetics. The synthesized Mt-VF complexes were characterized by XRD, FTIR, TGA, DSC etc. VF was found to be intercalated in the Mt layers. The release profile of the VF and Mt-VF complex in simulated gastric and intestinal fluids has been discussed. The release behaviour of VF from Mt-VF complexes appears to be sustained/extended for a period of 12 h and reaches upto 52 % in simulated gastric fluid and is stable in intestinal fluid where as pure VF completely gets released in 5.5 h and 3.5 h in simulated gastric and intestinal fluid respectively. Out of all kinetic models used to elucidate the drug release mechanism, the best fitting was observed for first order model. On the basis of present studies it can be stated that the synthesized Mt-VF complexes have the potential for developing in to a sustained release formulation for oral drug delivery of an anti-depressant drug VF. This shows a path which can reduce doses substantially from 4 times in 24 h to twice in 24 h.

* Corresponding Authors

E-Mail: monikadatta_chem@yahoo.co.in

[a] Analytical Research Laboratory, Department of Chemistry, University of Delhi, Delhi 110007, India

It is a GRAS grade FDA approved clay and has attracted great interest from researchers. It belongs to the 2:1 smectite group of clay minerals.

INTRODUCTION

Clay minerals possessing layered structure are known to exhibit properties such as good water absorption, swelling and cation exchange ability which are considered beneficial for the synthesis of pharmaceutical products, both as inactive and active substances.¹⁻³ Clay minerals being natural cation exchanger can bind with cationic drugs via electrostatic interaction. These properties have encouraged the use of clay minerals for developing drug delivery vehicle for extended release of drugs.⁴⁻¹⁰ Pharmaceutical preparations, using minerals as carrier-releasers of active ingredients, can generally be administered orally to the patient there by making them a preferred choice for oral drug delivery vehicle.¹¹

Montmorillonite (Mt), also known as medical clay, is a potent detoxifier that can adsorb dietary and bacterial toxins.¹²⁻¹⁴

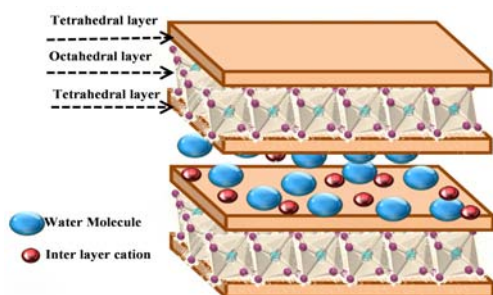


Figure 1. Structural representation of hydrated Mt general formula $M_{x+y}(Al_{2-x})(OH)_2(Si_{4-y}Al_y)O_{10}$

It has large specific surface area, good adsorption and cation exchange capacity. Mt is known to intercalate various protonated and hydrophilic organic molecules, which can be released in a controlled manner by replacement with other kind of cations in the release media.¹⁵⁻¹⁷ Drug intercalated Mt formulations offer a novel route to prepare organic and inorganic complexes that contain advantageous properties of both the inorganic host and organic guest in a single material.¹⁸⁻²⁰ (Fig. 1)

Belonging to the third generation antidepressant drugs Venlafaxine hydrochloride (Fig. 2) inhibits reuptake of serotonin, norepinephrine and, to a lesser extent, dopamine. It is a white crystalline solid which is highly soluble in water ($>500 \text{ mg mL}^{-1}$).²¹⁻²² Due to the short steady state elimination half-life (4-5 h) the drug has to be administered 2 to 3 times in 24 h so as to maintain required concentration of the drug in the blood plasma. The dose of VF ranges from 75 to 350 mg d^{-1} .²³ The available two formulations for this drug namely immediate and extended release formulations have various side effects and certain drawbacks such as, slow release characteristics, instability in high acidic conditions.²⁴ Therefore an effective oral drug delivery system is needed to overcome these drawbacks and to improve the clinical treatment process which is capable of maintaining the therapeutic concentration over a longer period of time. Therefore an oral drug delivery system with extended release characteristics can prove to be more patient compliant.²⁵⁻²⁶

The objective of the present work is to develop and characterize VF loaded Mt-VF complex as a controlled drug delivery system for oral administration of VF.

There is no report, to the best of our knowledge, on the preparation of VF intercalated Mt complexes for the oral extended delivery of VF.

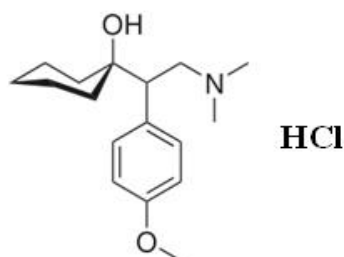


Figure 2. Structural representation of Venlafaxine hydrochloride (VF)

Therefore, the aim of our work was to undertake a systematic and detailed investigation on adsorption and optimization of conditions for preparing Mt-VF complexes for sustained release formulations. The effect of pH, time and initial drug concentration on drug intercalation capacity of Mt has been evaluated. Thus the developed Mt-VF complexes have the potential to be used as an oral extended delivery of VF for the patients requiring medicinal treatment around the clock.

EXPERIMENTAL

Materials

Montmorillonite (KSF) was procured from Sigma Aldrich (USA) and Venlafaxine hydrochloride (purity >98%) was gift from Ami life sciences Pvt. Limited, Maharashtra. Analytical grade sodium hydroxide, potassium dihydrogen phosphate, hydrochloric acid and potassium chloride for the preparation of drug release media were obtained from Merck Chemicals Ltd (India). Water used in the experiments was deionized and filtered (Milli-Q Academic, Millipore, France).

Effect of pH on absorption spectrum of VF

Initially the stability behaviour of VF was studied in the pH range 1-12 (Fig. 3).

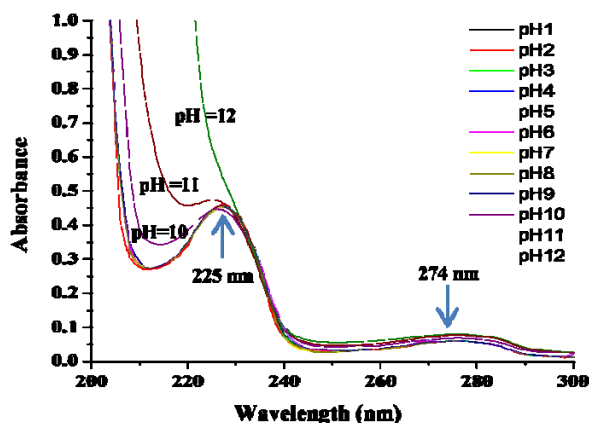


Figure 3. UV-Visible spectra of aqueous VF solution (10 ppm) showing effect of pH

Drug loading capacity of Mt for VF

In order to determine the conditions for maximum loading of VF on Mt, effect of various parameters such as contact time, pH and initial concentration of VF were investigated using batch extraction method. As the drug was not stable beyond pH 9 therefore the influence of pH on loading of VF on Mt was studied with in pH range of 1-9 at 25 °C. Initially a stock solution of the drug, 1000 $\mu\text{g mL}^{-1}$, was prepared. 5 mL of this solution containing 5000 μg of drug was taken in a 100 mL volumetric flask containing 100 mg of Mt. Then solution was maintained at various pH 1-9 and the volume was made upto 25 mL. The resulting dispersion was put on continuous mechanical shaking (Khera instruments).

The dispersion was centrifuged at 25,000 rpm for 30 min at room temperature (Sigma centrifuge). The free VF concentration in the supernatant was determined using UV-visible spectrophotometer (Analytic Jena) from the Lambert-Beer's plot and the percentage of the drug loaded was calculated using Equation (1)

$$\phi = \frac{C_i - C_e}{C_i} \quad (1)$$

where

C_i is the initial drug concentration (mg L^{-1}) and

C_e is the concentration of the drug (mg L^{-1}) in the supernatant at the equilibrium stage.

The amount of drug adsorbed q_e (mg g^{-1}) was calculated via the mass-balance relationship as per Equation (2)

$$q_e = (C_i - C_e) \frac{V}{m} \quad (2)$$

where

V (in L) is the volume of the reaction media and

m is the mass of Mt (in g) used for the studies.

The pH where the loading of drug on Mt was maximum was chosen to perform time dependent and adsorption kinetic studies in the time period of 0.25 h to 24 h, keeping all the other parameters constant.

Once the optimal time for highest uptake of drug was obtained, adsorption equilibrium studies of VF in the concentration range of 16 to 720 mg L^{-1} (400 μg -18000 μg) were carried out maintaining other obtained best pH and time.

Characterizations

The samples were analyzed and characterized using suitable analytical techniques discussed under appropriate headings.

UV-Visible spectrometry

UV-Visible absorbance of the supernatant solutions was measured at $\lambda_{\text{max}} = 225 \text{ nm}$ (UV-Visible spectrophotometer Analytic Jena) equipped with a quartz cell having a path length of 1 cm.

X-ray Diffraction

Powder X-ray diffraction (PXRD) measurements of samples were performed on a powder X-ray diffractometer (D8 DISCOVER BRUKER AXS, Germany) the measurement conditions were Cu α radiation generated at 40 kV and 40 mA as X-ray source $2\text{-}40^\circ$ (2θ) and step angle $0.02^\circ \text{ s}^{-1}$.

Thermal Analysis

The effect of Mt content on thermal stability of Mt-VF-complex was assessed by the thermogravimetric analyzer (TGA 2050 Thermal gravimetric Analyzer, Perkin Elmer).

The differential scanning calorimetric studies were conducted on DSC instrument (DSC Q200 V23.10 Build 79). The samples were purged with dry nitrogen at a flow rate of 10 mL min^{-1} , the temperature was raised at $5^\circ \text{ C min}^{-1}$.

Fourier-transformed infrared (FT-IR) spectrometry

FT-IR spectra was recorded with an FTIR spectrophotometer (Perkin Elmer, Spectrum BxFTIR Spectrometer) using the KBr (Merck, Germany) disc method.

Scanning electron microscopy (SEM) with EDS

Scanning Electron Microscopic (SEM) images were recorded to study the surface morphology of Mt and Mt-VF complex. Sample was mounted on carbon tape on a stub; sputter coated with gold in a vacuum evaporator and images were recorded using a scanning electron microscope (model, JEOL JSM-6610LV).

Behaviour of drug under in vitro conditions

Kinetics of drug release under in vitro conditions was performed using USP six stage dissolution rate test apparatus (DISSO 8000, Lab India, India) with the dialysis bag technique. Simulated gastric fluid was prepared by mixing 250 mL of 0.2 M HCl and 147 mL of 0.2 M KCl (buffer solution of pH 1.2). Simulated intestinal fluid was prepared by mixing 250 mL of 0.1 M KH_2PO_4 and 195.5 mL of 0.1 M NaOH (buffer solution of pH 7.4). Dialysis bags were equilibrated overnight with the dissolution media prior to experiments. A known amount of sample is placed in the dialysis bag containing 5 mL of dissolution medium. The drug loaded dialysis bag was placed into the receptor compartment containing 500 mL dissolution medium with constant stirring (80 rpm) maintained at $37 \pm 0.5^\circ \text{ C}$. An aliquot (5 mL) was withdrawn at regular interval of time followed by replenishment with equal volume of dissolution

medium to maintain same volume of dissolution medium. The extracted aliquots were analyzed for its drug content using UV spectrometer at 225 nm (calibration plot of standard drug solutions were prepared in the same releasing media). The above mentioned procedure is repeated for every sample (pure VF, Mt-VF complex) in simulated gastric fluid and simulated intestinal fluid.

To analyze the in vitro release data, various kinetic models including Zero order, First-order, Higuchi and Korsmeyer-Peppas model has been used to describe the release kinetics.²⁷⁻²⁹

RESULTS AND DISCUSSION

Interaction of VF at different pH values

Mt has the ability to swell on coming into contact with water and the exchangeable cations/drugs diffuse into the water phase [30]. To start with the experiment, effect of pH on the VF molecule was investigated in the range of 1-12. It was found that drug maintains its absorption maxima (Fig. 3) within the experimental pH range of 1-9. The UV absorption spectra of VF show two absorption peaks at 225 nm and 274 nm corresponding to different electronic transitions of the molecule.³¹⁻³³ In subsequent studies, wavelength of 225 nm has been selected for quantitative estimation of VF.

The pH of the solution has always played a crucial role in adsorption process.³⁰ The loading of VF in Mt was found to increase from 1750 μg to 2400 μg (35 % to 48 %) in the pH range of 1-6 and then decrease to 1800 μg (36 %) in the pH range of 7-9 (Fig. 4).

This could be explained on the basis that at lower pH loading of drug is less due to the competition between the cationic drug and H^+ ions present as exchangeable ion in Mt where as in the slightly acidic medium around pH=6, VF will be positively charged because of the presence of tertiary amino groups in its molecular structure³⁴ therefore the amount of VF loaded on Mt increases slightly.

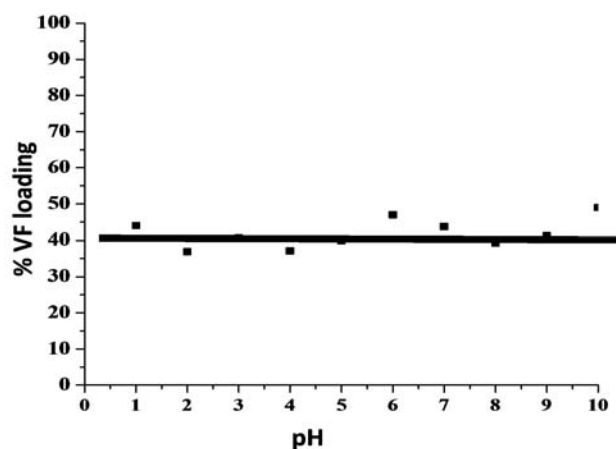


Figure 4. VF loading on Mt as a function of pH

The maximum drug loading was observed at pH=6 (48 %) which was also the natural pH of the drug solution used in the present work. Therefore, the subsequent studies were carried out at pH=6.

Effect of time on loading of VF on Mt

Intercalation of VF in Mt is a rapid process, due to occurrence of ion-exchange reaction between the interlayer Na⁺ ions and cationic VF molecules at pH= 6 (Fig. 5).

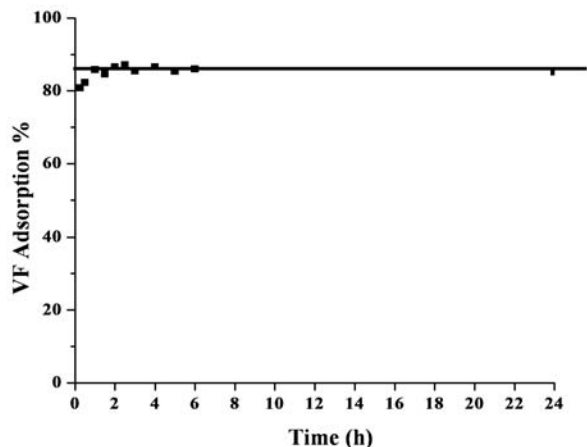


Figure 5. Effect of contact time on loading of VF on Mt.

Initially 4111 µg (80 % of 5000 µg) of VF was loaded within 0.5 h of interaction time, which increased to 4353 µg (87 % 5000 µg) in 2.5 h and remained almost constant 4300 µg (86 % of 5000 µg) up to 6 h and tends to decrease up to 4258 µg (85 % of 5000 µg) in further 18 h. Therefore, for further experiments in our studies, reaction time was set to 2.5 h in order to have maximum loading.

Effect of initial VF concentration on loading on Mt

The loading of VF in Mt layers is also affected by its initial amount present in the solution.

As the VF amount in the solution increases from 400 µg to 18000 µg (40 - 720 mg L⁻¹), the amount of VF loaded on Mt increases from 338 µg to 1758 µg (84.6 % to 94 %) (Fig. 6). Therefore, the optimal concentration was found to be 1800 µg of VF/100 mg of Mt for further studies and characterizations.

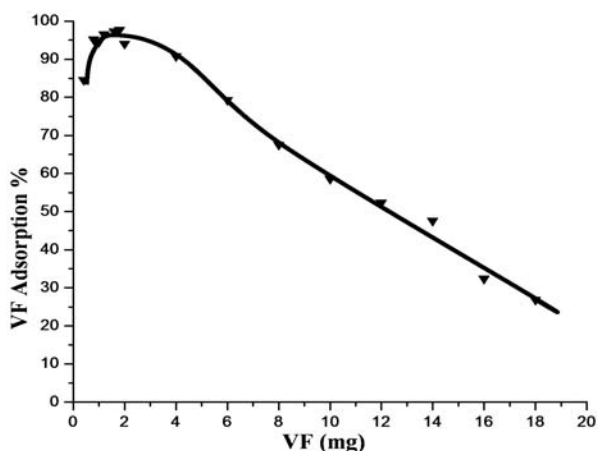


Figure 6. Effect of initial VF concentration on loading on Mt

Kinetics of VF Adsorption

In order to optimize the design of an adsorption system of VF on Mt, it is important to establish the most appropriate correlations for the equilibrium data for the system. In this respect two kinetic models including pseudo first order and pseudo-second order models have been applied to determine the adsorption mechanism.³⁵

Pseudo-first-order model

Pseudo-first-order equation can be expressed as below Equation (3): where k_1 is the pseudo-first-order rate constant (min⁻¹), q_t is the amount of drug adsorbed (mg g⁻¹) at different times t , q_1 is the maximum adsorption capacity (mg g⁻¹) for pseudo first- order adsorption. Plots of $1/q_t$ versus $1/t$ for the adsorption of VF on Mt surface were employed to generate the intercept values of $1/q_1$ and the slope of k_1/q_1 (Fig. 7). The values of k_1 , q_1 and the correlation coefficients are given in Table 1.

$$\frac{1}{q_t} = \frac{k_1}{q_1} \frac{1}{t} + \frac{1}{q_1} \tag{3}$$

Figure 7. Pseudo first order kinetic model for VF adsorption on Mt surface

Pseudo second order model

The pseudo-second-order kinetic equation can be represented as Equation (4): where k_2 is the pseudo-second order rate constant; q_2 is the maximum adsorption capacity (mg g⁻¹) for the second order adsorption process. The plots of t/q_t versus t for VF adsorption on Mt are given in Fig. 8. From the slope and intercept values, q_2 and k_2 values were calculated with results given in Table 1.

$$\frac{t}{q_t} = \frac{1}{k_2 q_2^2} + \frac{t}{q_2} \tag{4}$$

Figure 8. Pseudo second order kinetic model for VF adsorption on Mt

Table 1. Kinetic parameters for the adsorption of VF on Mt surface

Pseudo first order			Pseudo second order		
k_1 , min ⁻¹	q_1 , mg g ⁻¹	R_1^2	k_2 , g mg min ⁻¹	q_2 , mg g ⁻¹	R_2^2
1.132	43.25	0.840	0.0428	43.04	0.999

Adsorption Isotherm for VF on Mt surface

The adsorption isotherm of VF on Mt surface obtained by plotting the amount of VF adsorbed by Mt (q_e , mg g⁻¹) vs equilibrium concentration of VF (C_e , mg L⁻¹) is shown in Fig. 9.

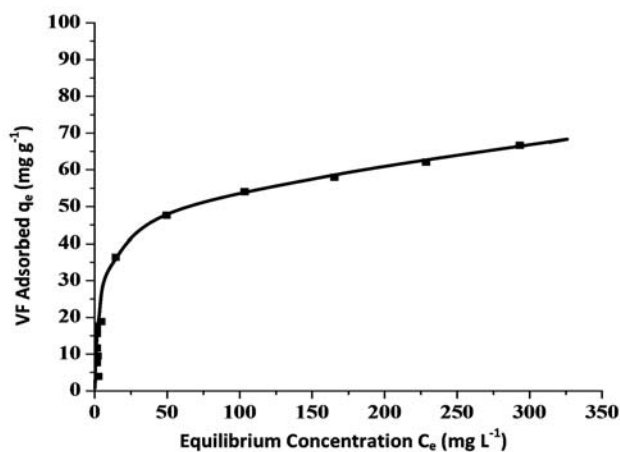


Figure 9. Adsorption isotherm of VF on Mt surface

The Langmuir (Equation-5) and Freundlich (Equation-6) adsorption isotherms were applied to evaluate the adsorption data which correspond to homogenous and heterogeneous adsorbent surfaces respectively.³⁰ The equations can be expressed as follows:

$$\frac{C_e}{q_e} = \frac{1}{q_m K_L} + \frac{C_e}{q_m} \quad (5)$$

$$\ln q_e = \ln K_f + n_f \ln C_e \quad (6)$$

where

q_e is the equilibrium VF concentration on the Mt surface (mg g^{-1}),

C_e is the equilibrium VF concentration in solution (mg L^{-1}),

q_m the monolayer adsorption capacity (mg g^{-1}), and

K_L is the Langmuir adsorption constant (L mg^{-1}).

In case of Freundlich adsorption isotherm,

K_f (mg g^{-1}) and n_f are considered as relative adsorption capacity and adsorption intensity respectively.

The values of q_m and K_L were computed from the slope and intercept of the linear plot of C_e/q_e versus C_e (Fig. 10) and are presented in Table 2.

Table 2. Isotherm constant for VF adsorption on Mt surface

Linear form of Langmuir		Linear form of Freundlich	
$q_m, \text{mg g}^{-1}$	67.11	$K_f, \text{mg g}^{-1}$	8.496
K_L	0.064	n_f	0.3873
R^2	0.989	R^2	0.7921

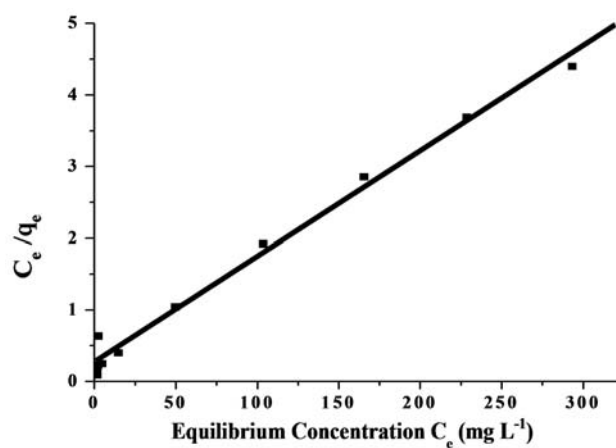


Figure 10. Linear form of Langmuir adsorption isotherm for VF on Mt

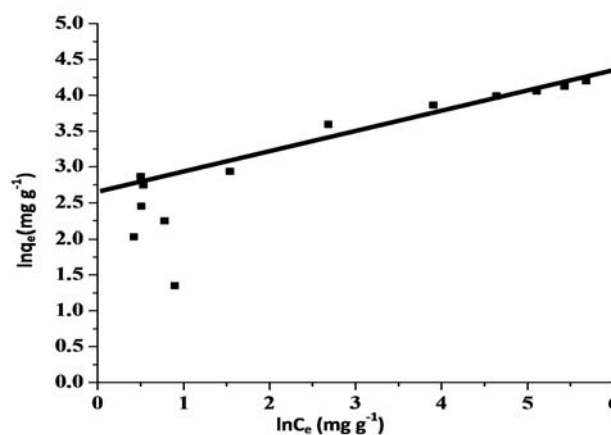


Figure 11. Linear form of Freundlich adsorption isotherm for VF on Mt

The linear form of Langmuir isotherms seems to produce a better fit in comparison with linear form of Freundlich isotherm (Fig. 11). The essential characteristics of the Langmuir equation can be expressed in terms of a dimensionless separation factor R_L as Equation-7:

$$R_L = \frac{1}{1 + K_L C_e} \quad (7)$$

The value of R_L indicates the shape of the isotherm to be either unfavorable ($R_L > 1$), linear ($R_L = 1$), favourable ($0 < R_L < 1$) or irreversible ($R_L = 0$) thereby indicates the nature of the favorability adsorption process and its feasibility. The results of R_L values were in the range of 0.494-0.023 indicate that the favourable adsorption of VF on Mt.³⁶

According to Freundlich equation, K_f value is 8.496 mg g^{-1} at 25°C . It can be said that the values of n_f equal to 0.3873 is smaller than 1, reflecting the favourable adsorption.

XRD Studies

The physical status of pure VF, Mt, Mt-VF complex has been compared with the help of XRD (Fig. 12). Pure VF shows strong diffraction peaks at $2\theta = 6.5^\circ, 8.5^\circ, 10.3^\circ, 12.8^\circ, 13.6^\circ, 15.6^\circ, 16.5^\circ, 19.1^\circ, 20.4^\circ, 21.2^\circ, 21.9^\circ, 25.1^\circ, 28.7^\circ, 31.2^\circ, 31.7^\circ, 35.3^\circ$ well supported by literature.³⁷

The XRD pattern of pristine Mt shows characteristic diffraction peak at 2θ value 6.4° corresponding to 001 plane with d value of 14.2 \AA .

In the case of Mt-VF complex an increase in intensity of 001 plane along with the shift in the 2θ value, from 6.02° to 5.5° , was observed. According to Bragg's law, shift in 2θ value from higher diffraction angle to lower diffraction angle is indicative of increase in d spacing i.e., from 14.2 \AA to 16 \AA ³⁸⁻⁴⁰ which can be related to the successful intercalation of VF in the Mt layers. Moreover the peaks at $8.5^\circ, 20.4^\circ, 21.8^\circ, 26.3^\circ$ indicates the presence of VF in the synthesized Mt-VF complex.

Subtracting the Mt layer thickness (9.6 \AA) from the d spacing (16 \AA) of the Mt-VF complex, the Mt layer thickness was estimated to be 6.4 \AA .³⁵ This data suggest the replacement of interlayer hydrated cations with monolayer the VF molecules parallel to the Mt layers is highly possible.⁴¹

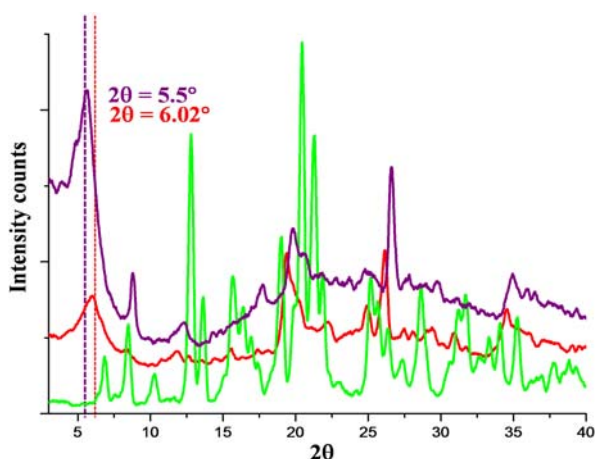


Figure 12. XRD patterns for Pure VF, Mt, Mt-VF complex.

FTIR Studies

In order to confirm the presence of VF within the interlayer region of the Mt, FTIR spectra were recorded in the region $400\text{--}4000 \text{ cm}^{-1}$.

In the FT-IR spectrum of Mt the band at 3436 cm^{-1} and 3641 cm^{-1} has been assigned to H-O-H stretching vibrations from interlayer water and Si-O-H stretching vibrations of the structural OH group. The broadness around $3496\text{--}3093 \text{ cm}^{-1}$ of the structural -OH band are mainly due to contributions of several structural -OH groups occurring in the Mt. The absorption band at 1645 cm^{-1} corresponds to H-O-H bending mode of adsorbed water.^{7,42}

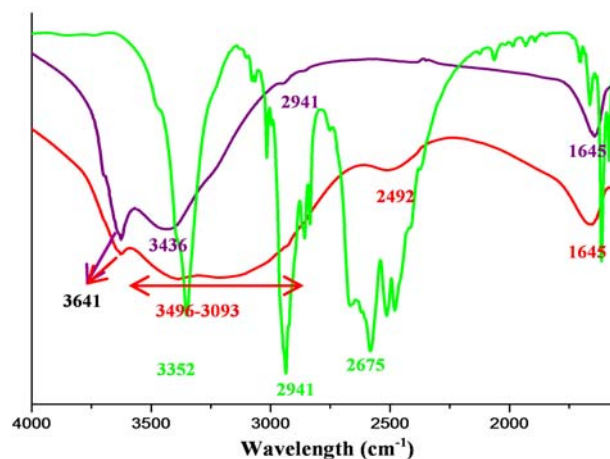


Figure 13. FTIR spectra of Pure VF, Mt, Mt-VF complex.

In the FTIR spectrum of the pure VF, appearance of absorption band at 3352 cm^{-1} corresponds to the stretching vibrations of hydroxyl group and band at 2941 cm^{-1} correspond to the stretching vibrations of aromatic CH present in VF.³⁴ However few characteristic bands around $2675\text{--}2480 \text{ cm}^{-1}$ have been observed but no vibrational mode have been assigned in literature as well.^{7,34}

In case of Mt-VF complex the vibrational bands 3436 cm^{-1} and 3641 cm^{-1} has been assigned to H-O-H stretching vibrations from interlayer water and Si-O-H stretching vibrations of the structural OH group but the broadness of this peak decreases as compared to Mt therefore decreasing the number of -OH stretching vibrations contributing to this peak indicating the intercalation of the VF (as confirmed by XRD) into the interlayer region has displaced the water molecules. The presence of functional groups of VF in the Mt-VF complex on the surface of Mt is also suggested by peak about 2941 cm^{-1} characteristic of the aliphatic C-H symmetric stretch of aromatic group of VF.

TGA Studies

Pristine Mt, pure VF and Mt-VF complex were characterized by TGA to evaluate their thermal behavior.

Pure Mt shows mass loss of 18 % from $30 \text{ }^\circ\text{C}$ to $140 \text{ }^\circ\text{C}$ and is attributed to the loss of adsorbed and interlayer water, with an endothermic peak in the DTA curve around $80 \text{ }^\circ\text{C}$. Mass loss in the temperature range from $600\text{--}750 \text{ }^\circ\text{C}$ is due to the loss of hydroxyl groups in the aluminosilicate structure and the structure of the Mt layers collapses, also indicated by a broad endothermic peak in DTA curve of Mt at $600 \text{ }^\circ\text{C}$.⁴³⁻⁴⁴

The pure VF shows two thermal decomposition stages. In the DTA curve for pure VF, a sharp endothermic peak at $218 \text{ }^\circ\text{C}$ was observed without any weight loss in TGA which corresponded to the melting point of VF. The drug show a sharp weight loss ($\sim 99 \%$) at around $230\text{--}320 \text{ }^\circ\text{C}$ resulting in a strong endothermic peak in DTA curve at $297 \text{ }^\circ\text{C}$ followed by a broad exotherm at $600 \text{ }^\circ\text{C}$ corresponding to decomposition of VF.⁴⁵

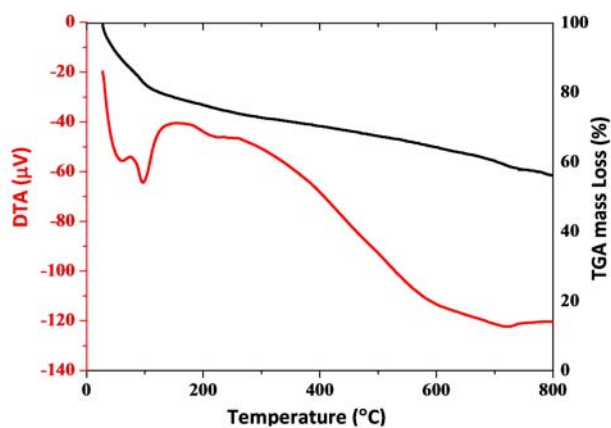


Figure 14a. TGA-DTA curves of Montmorillonite

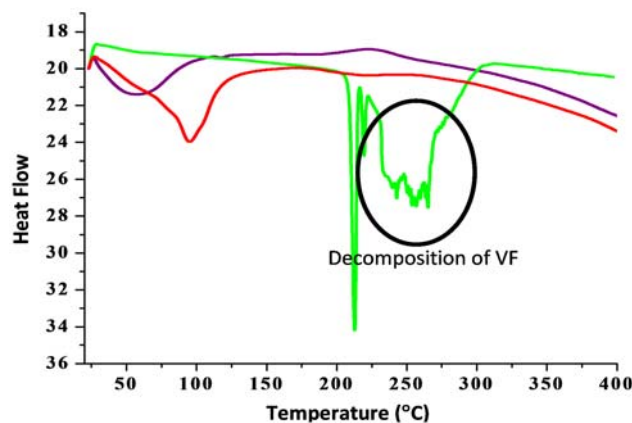


Figure 15. DSC curves of Pure VF, Montmorillonite and Mt-VF complex

Mt shows an exothermic peak around 90 °C suggesting the dehydration of adsorbed water from the surface of Mt.

In case of Mt-VF complex a broad endotherm was appeared in the region of 60 °C to 100 °C which might corresponds to dehydration of surface water. In the temperature region of 200 °C to 300 °C, an exotherm might be related to the decomposition of VF within Mt layers was observed. (Fig. 15).

Scanning Electron Microscopy with Energy dispersive X-Ray Analysis

To analyze the surface morphology of Mt-VF complex Scanning Electron Microscopic with Energy dispersive X-Ray Analysis was performed. The surface of Mt has a layered smooth surface whereas the Mt-VF complex has layered but rough surface indicating the presence of VF molecule on the surface.

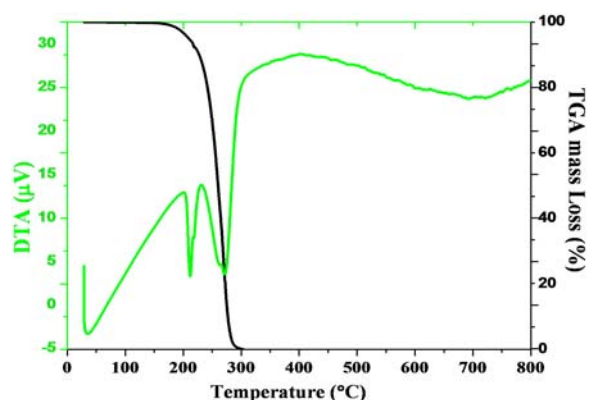


Figure 14b. TGA-DTA curves of Pure VF

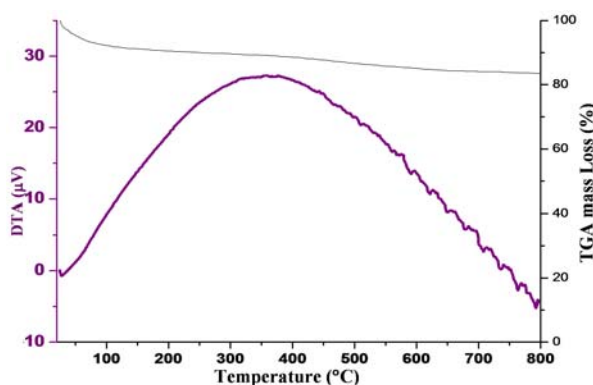


Figure 14c. TGA-DTA curves of Mt-VF complex.

In case of Mt- VF complex the single step mass loss of 18 % in the range from 205 °C to 700 °C suggests the decomposition of intercalated VF.

DSC Studies

The physical state and crystallinity of the drug in case of Mt-VF complex have been investigated and compared to pure VF and Mt. Sharp endotherm at 212 °C and 250 °C has been observed for VF corresponding to the melting and decomposition of the pure compound.^{45,46}

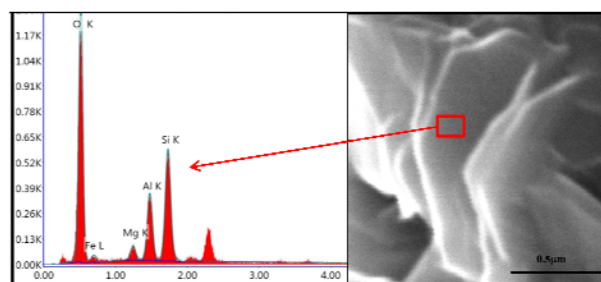


Figure 16a. SEM image and EDX graph of montmorillonite

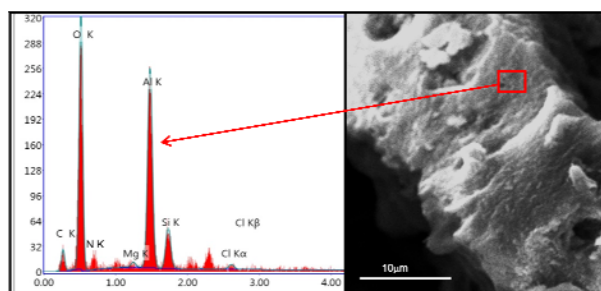


Figure 16b. SEM image and EDX graph of Mt-VF complex

High % content of oxygen, silicon and aluminum is observed in case of Mt where as in Mt-VF complex additional peaks of carbon nitrogen and chlorine are present along with oxygen, silicon and aluminum EDX analysis (Figs. 16a and 16b and Table 3). Since, the drug contains chlorine, nitrogen and carbon therefore it can be taken as an evidence for the presence of drug on the Mt-VF complex.

Table 3. Elemental analysis of Mt and Mt-VF complex

Element	Mt		Mt-VF complex	
	Weight%	Atomic%	Weight %	Atomic %
Fe	05.68	01.99	00.00	00.00
Mg	02.39	01.93	00.00	00.00
C	00.00	00.00	15.25	21.98
O	60.3	73.73	54.30	58.74
N	00.00	00.00	00.57	00.41
Al	11.40	08.26	23.20	14.88
Si	20.23	14.09	05.72	03.52
Cl	0.00	0.00	00.95	00.46
Total	100.00	100.00	100.00	100.00

Drug Release Profile

VF is well absorbed and extensively metabolized in the liver.⁴⁷ Therefore it is necessary to study the release profile of the selected Mt-VF-complex in simulated gastric and intestinal fluid, in comparison with the release profile of pure drug under identical experimental conditions.

In stimulated gastric fluid the pure VF shows a rapid burst (releasing 35 % of the drug) in the initial 0.5 h followed by 100 % release of the drug over a period of 5.5 h. In case of Mt-VF complex a sustained release of VF in the gastric fluid (HCl,pH 1.2) was observed. Within initial 2 h, only 7.3 % of VF was released which approaches to 48 % in 7 hours and 53 % over a period of 10 h (Fig.17). The release in acidic media may be due to cation exchange with H⁺ ions from the media, being smaller in size, they can penetrate deep into the Mt layers and results in high ion exchange process (Fig. 17).

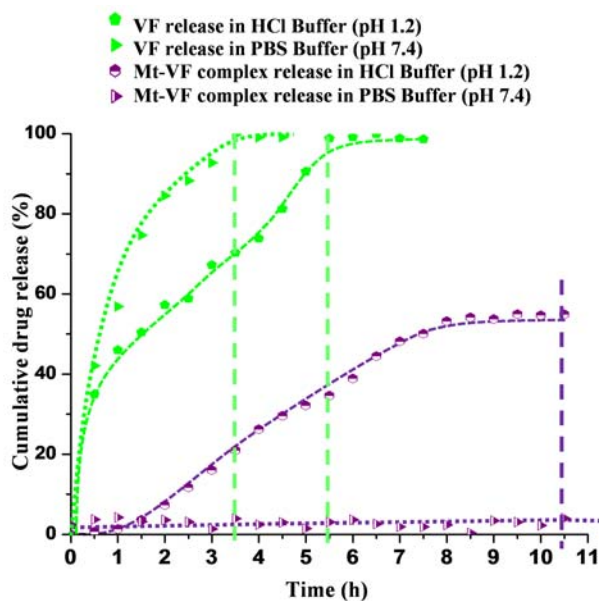


Figure 17. Release profile of pure VF and Mt-VF complex in HCl buffer pH 1.2 and PBS pH 7.4

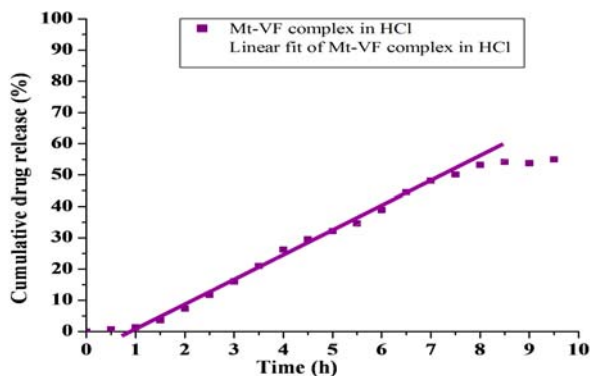


Figure 17a. Zero order kinetic model of Mt-VF complex in simulated gastric fluid

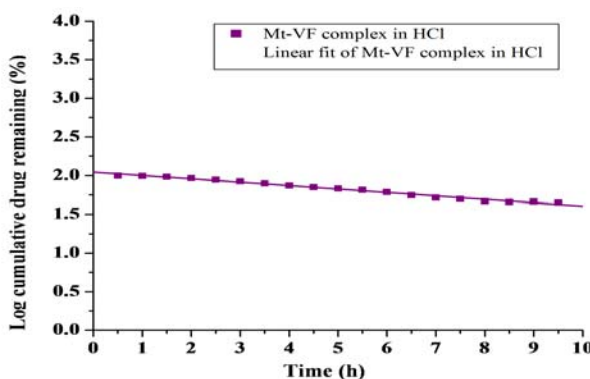


Figure 17b. First order kinetic model of Mt-VF complex in simulated gastric fluid

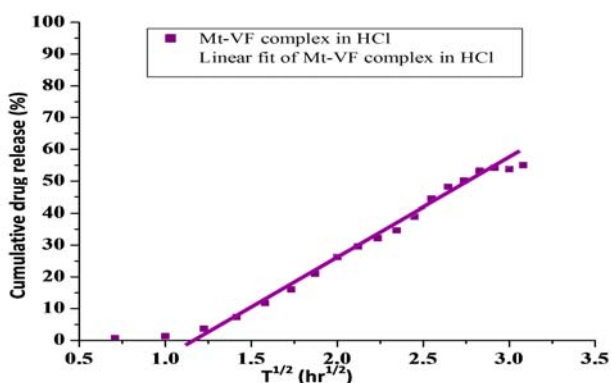


Figure 17c. Higuchi kinetic model of Mt-VF complex in simulated gastric fluid

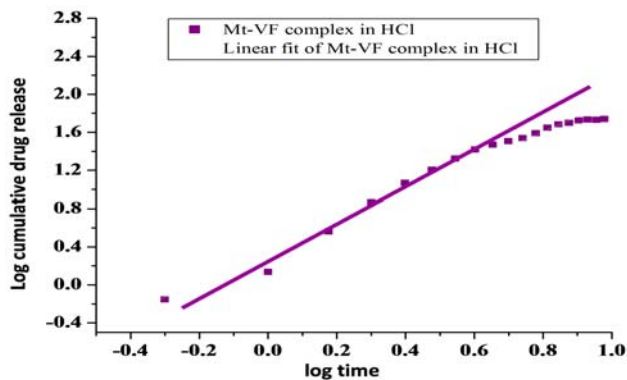


Figure 17d. Korsmeyer-Peppas kinetic model of Mt-VF complex in simulated gastric fluid

Table 4. Release kinetics of Mt-VF complex in simulated gastric fluid (HCl, pH 1.2)

Release media	Zero order, $C=K_0t$		First order, $\log C=\log C_0-k_1t/2.303$		Higuchi, $Q=K_Ht^{1/2}$		Korsmeyer-Peppas, $M_t/M_\infty=kt^n$		
	R^2	K_0, h^{-1}	R^2	K_1, h^{-1}	R^2	$K_H^{(-1/2)}$	R^2	n	K_{kp}, h^{-n}
HCl pH 1.2	0.979	6.871	0.985	0.101	0.972	27.36	0.971	1.5	2.215

In stimulated intestinal fluid, PBS (pH 7.4) the pure VF shows a rapid burst (releasing 42 % of the drug) in the initial 0.5 h followed by 100 % release of the drug over a period of 3.5 h. In case of Mt-VF complex no release of VF was observed up to 10.5 h. This indicates that VF release was greatly influenced by the pH of the releasing media.³⁵

In vitro drug release data suggest that the synthesized Mt-VF complex are able to extend the release of VF in gastric fluid (acidic media, pH 1.2) beyond 8 h. As a result more amounts is expected to reach liver for its complete absorption.⁴⁸

The release data of VF form Mt-VF complex were fitted by zero order (Fig. 17a), first-order kinetics (Fig. 17b), Higuchi (Fig. 17c) and Korsmeyer-Peppas models (Fig. 17d) and the values of release kinetics constants in simulated gastric (HCl, pH 1.2) fluid are summarized in Table 4. In (HCl, pH 1.2) the first order equation gave the best representation of the release data.⁴⁹

CONCLUSIONS

VF sustained release formulation was prepared successfully using natural clay mineral Mt as a host to retard the drug release. Intercalation of VF in Mt layers was indicated by XRD. The adsorption isotherms of VF on Mt were best fitted by the Langmuir model and the adsorption kinetics followed the pseudo second-order kinetic model. Drug release kinetics of this formulation corresponds best to first order model in gastric media (pH 1.2). In vitro drug release data suggest that the synthesized Mt-VF complex is capable of gradual drug release over a longer period of time in gastric media (pH 1.2) as compared to pure drug thereby increasing the availability of the drug for absorption in liver. Thus the obtained results are proposing a possibility of new formulation suitable as an extended delivery carrier of venlafaxine hydrochloride.

ACKNOWLEDGEMENT

Authors are thankful to the USIC, University of Delhi for providing instrumentation facilities and CSIR for providing financial assistance to one of the authors, Shilpa Jain.

REFERENCES

- Yuan, Q., Shah, J., Hein, S., Misra, R.D.K., *Acta Biomater.*, **2010**, *6*, 1140.
- Ricka, J., Tanaka, T., *Macromolecules*, **1984**, *17*, 2916.
- Hirokawa, Y., Tanaka, T., *J. Chem. Phys.*, **1984**, *81*, 6379.
- Sorby, D.L., *J. Pharm. Sci.*, **1965**, *54*, 677.

- Sorby, D.L., Liu, G., *J. Pharm. Sci.*, **1966**, *55*, 504.
- Aguzzi, C., Cerezo, P., Viseras, C., Caramella, C., *Appl. Clay Sci.*, **2007**, *36*, 22.
- Peppas, N.A., *Int. J. Pharm.*, **2004**, *277*, 11.
- Nair, L.S., Laurencin, C.T., *Prog Polym Sci.*, **2007**, *32*, 762.
- Coviello, T., Matricardi, P., Marianecchi, C., Alhague, F., *J. Control. Release.*, **2007**, *119*, 5.
- Wai, K.N., Banker, G.S., *J. Pharm. Sci.*, **1966**, *55*, 1215.
- Carretero, M. I., Pozo, M., *Appl. Clay Sci.*, **2009**, *46*, 73.
- Lee, Y.H., Kuo, T.F., Chen, B.Y., Feng, Y.K., Wen, Y.R., Lin, W. C., Lin, F.H., *Biomed. Eng. Appl., Basis Commun.*, **2005**, *17*, 72.
- Feng, S.S., Mei, L., Anitha, P., Gan, C.W., Zhou, W., *Biomaterials*, **2009**, *30*, 3297.
- Dong, Y., Feng, S.S., *Biomaterials*, **2005**, *26*, 6068.
- Chen, Y.M., Zhou, A.N., Liu, B., Liang, J., *Appl. Clay Sci.*, **2010**, *49*, 108.
- Joshi, G.V., Kevadiya, B.D., Patel, H.A., Bajaj, H.C., Jasra, R.V., *Int. J. Pharm.*, **2009**, *374*, 53.
- Meng, N., Zhou, N.L., Zhang, S. Q., Shen, J., *Int. J. Pharm.*, **2009**, *382*, 45.
- Joshi, G.V., Patel, H.A., Bajaj, H.C., Jasra, R.V., *Coll. Polym. Sci.*, **2009**, *287*, 1071.
- Joshi, G.V., Kevadiya, B.D., Bajaj, H.C., *Micropor. Mesopor. Mater.*, **2010**, *132*, 526.
- Chen, B.Y., Lee Y.H., Lin W.C., Lin F.H., Lin K.F., *Biomed. Eng. Appl., Basis Commun.*, **2006**, *18*, 30.
- Entsuah, R., Chitra, R., *Psychopharmacol. Bull.*, **1997**, *33*, 671.
- Klamerus, K.J., Maloney, K., Rudolph, R.L., Sisenwine, S.F., Jusko, W.J., Chiang, S.T., *J. Clin. Pharmacol.*, **1992**, *32*, 716.
- Haskins, J.T., Moyer, J.A., Muth, E.A., Sigg, E.B., *Eur. J. Pharmacol.*, **1985**, *115*, 139–146.
- Olver, J.S., Burrows, G.D., Norman, T.R., *CNS Drugs*, **2001**, *15*(12), 941.
- Patel, H. A., Shah, S., Shah, D.O., Joshi, P.A., *Appl. Clay Sci.*, **2011**, *51*, 126.
- Rx list, the internet drug index, <http://www.rxlist.com/effexor-xr-side-effects-drug-center.htm>
- Dash, S., Murthy, P.N., Nath, L., Chowdhury, P., *Acta Pol. Pharm. Drug. Res.*, **2010**, *67*, 217.
- Singhvi, G., Singh, M., *Int. J. Pharm. Stud. Res.*, **2011**, *January-March*, 77.
- Costa, P., Lobo, J.M.S., *Eur. J. Pharm. Sci.*, **2001**, *13*, 123.
- Raghvendra, R. S., *Int. J. Pharm. Sci. Rev. Res.*, **2012**, *17*, 51.
- Lavanya, K., Sunitha, P., Kumar, A., Ramana, K.V., *Int. J. Pharm. Qual. Ass.*, **2013**, *14*, 1.
- Rao, K.S., Jadhav, S., Patil, P., Dattatraya, B.U., *Int. Res. J. Pharm.*, **2011**, *2*, 261.
- Patel, B., Patel, J., Banwait, H., Darji, N., Patel, D., Gabhawala, A., Patel, B., Patel, M., *Int. J. Inst. Pharm. Life Sci.*, **2011**, *1*.

- ³⁴Shah, S., Pal, A., Kaushik, V. K., Devi, S., *J. Appl. Polym. Sci.*, **2009**,112, 2876.
- ³⁵Seema, Datta, M., *Eur. Chem. Bull.*, **2013**, 2, 942.
- ³⁶Alzaydien, A.S., *Am. J. Environ. Sci.*, **2009**, 5, 197.
- ³⁷Aronhime, J., Dolitzky, B.Z., Nisnevish, G., Wize, S., US patents US20020143211 A1 Oct 3, **2002**.
- ³⁸Das, P.R., Nanda, R.M., Behara, A., Nayak, P.L., *Int. Res. J. Biochem. Bioinform.*, **2011**,1,35.
- ³⁹Olad, A., Advances in Diverse Industrial Applications of Nanocomposites, Chapter 7, 1st edition, India: Intech, **2011**,113. ISBN: 978-953-307-202-9,
- ⁴⁰Zampori, L., Stampino, P.G., Cristiani, C., Cazzola, P., Dotelli, G., *Appl. Clay Sci.*, **2010**, 50, 266.
- ⁴¹Sivalakshmi, A., Vyas, K., Rao, S.M., Reddy, G.O., *Acta Cryst. Sect. E*. **2002**, 58, 1072-1074
- ⁴²Abdeen, R., Salahuddin, N., *J. Chem.*, **2013**, 1-9.
- ⁴³Entsuah, R., Chitra, R., *Psychopharmacol. Bull.*, **1997**, 33, 671.
- ⁴⁴He, H., Ding, Z., Zhu, J., Yuan, P., Xi, Y., Yang, D., Frost, R.L., *Clays Clay Miner.*, **2005**, 53, 287.
- ⁴⁵Roy, S., Aitipamula, S., Nangia, A. *Cryst. Growth Design*, **2005**, 5, 2268.
- ⁴⁶Bernardi, L.S., Oliveira, P.R., Murakami, F.S., Silva, M.A.S., Borgmann, S.H.M., Cardoso, S.G., *J. Therm. Anal. Calorim.*, **2009**,97, 729.
- ⁴⁷<http://www.healthcentral.com/druglibrary/408/effexor> xr-clinical_pharmacology.html
- ⁴⁸Singh, G., Ghosh, B., Kaushalkumar, D., Somsekhar, V., *AAPS PharmSciTech*, **2008**, 9(3), 791.
- ⁴⁹Ajit, I., Senthil, A., Rahul, B., Narayanaswamy, V.B., *Int. J. Pharm.*, **2012**, 3, 226.

Received: 31.03.2014.

Accepted: 28.05.2014.